

Oxygen-ion implanted silicon microring resonator for high-speed all-optical switching

Michael Först(1), Jan Niehusmann (1), Tobias Plötzing (1),

Thorsten Wahlbrink (2), Christian Moormann(2), and Heinrich Kurz (1,2)

1) Institut für Halbleitertechnik, RWTH Aachen University, 52074 Aachen, Germany,

Email: foerst@iht.rwth-aachen.de

2) Advanced Microelectronic Center Aachen (AMICA), AMO GmbH, 52074 Aachen, Germany

Abstract: *Ultrafast all-optical switching is demonstrated in an oxygen-ion implanted silicon-on-insulator microring resonator. The spectral response of the device is rapidly modulated via femtosecond optical excitation and subsequent recombination of charge carriers at artificially introduced ultrafast recombination centers. At an implantation dose of $1 \times 10^{12} \text{ cm}^{-2}$ the carrier lifetime is reduced to 55 ps which facilitates optical switching of signal light in the $1.55 \mu\text{m}$ wavelength range at modulation speeds larger than 5 Gbit/s.*

Introduction

Silicon-on-insulator (SOI) technology is a promising platform to realize cost-efficient CMOS-compatible integrated photonic on-chip components. Among a variety of passive and active photonics devices demonstrated in recent years (see, e.g., Ref. 1 for an overview), compact microring resonators fabricated from Si strip waveguides have gained noticeable attention [2, 3]. They appear specifically attractive for active photonic switching, since their spectral transmission characteristics are very sensitive to minimal modifications of the optical phase [4].

In the case of all-optical switching, the transmission of a photonic device can be modulated by the optical Kerr effect or by photoexcitation of electron-hole pairs where the latter modify the silicon dielectric function based on the plasma dispersion effect [5]. All-optical carrier-based switching in a silicon microring resonator has been demonstrated via vertical out-of-plane optical excitation and via resonantly in-plane coupled excitation upon linear absorption and nonlinear two-photon absorption, respectively [6, 7]. The switching speed of this approach is determined by the effective free carrier lifetime. Bulk and surface recombination processes in the silicon waveguide and at sidewalls as well as carrier diffusion out the modal area are the dominating processes [8]. They limited the switching time to approximately 450 ps in both experiments.

An increase of switching speed requires the artificial reduction of the effective free carrier lifetime in the photonic device. One alternative is the incorporation of lateral p-i-n structures to the silicon waveguides for electrical carrier sweep out [9, 10, 11]. By this means, the modulation time of a microring resonator could be decreased to about 120 ps [12]. On the other hand, ion-implantation is a well known process to reduce ef-

fective free carrier lifetimes in semiconductors. Defect states artificially introduced into the crystalline semiconductor act as trapping centers for fast electron-hole pair recombination [13]. It was recently shown that He-ion implantation can decrease the free carrier lifetime in large area Si rib waveguides down to the nanosecond scale [14]. The result was an enhancement Raman amplification in that experiment.

In this contribution, we demonstrate that O⁺-ion implantation of silicon waveguides is an extremely valuable approach for high-speed switching applications in SOI microring resonators. Compared to incorporating p-i-n junctions to the resonator waveguide, the fabrication of the final device benefits from relaxed processing requirements – since only one sort of ions has to be implanted and masking issues require less accuracy. Even higher switching speeds appear feasible via the implantation approach, since the free carrier lifetime can be precisely tailored down to the few-picosecond range via the chosen implantation dose.

Device fabrication

The investigated device is a waveguide bus-coupled silicon microring resonator fabricated from an SOI substrate. All waveguides are 300 nm high and 400 nm wide, the resonator radius is $5 \mu\text{m}$, and the coupling gap between resonator and adjacent straight waveguides is 300 nm. The photonic structure was defined by electron beam lithography (EBL) using hydrogen silsesquioxane (HSQ) as resist. Pattern transfer is achieved by HBr inductive coupled reactive-ion etching.

To reduce the free carrier lifetime in the microring resonator, the device was implanted with O⁺ ions at an energy of 120 keV and a dose of $1 \times 10^{12} \text{ cm}^{-2}$. These parameters were chosen for the following reasons: (i) Taking into account the residual 100 nm thick HSQ EBL resist layer on top of the waveguide, the depth profile of defect states is calculated to be centered midway the waveguide height. (ii) According to previous studies on the implantation of bulk silicon, an implantation dose in the range of $1 \times 10^{12} \text{ cm}^{-2}$ should result in carrier lifetimes clearly below 100 ps [13]. To protect the several millimeter long bus waveguides from implantation, the sample was covered by an additional 900 nm thick SiO₂ layer prior to this process except of a $50 \times 50 \mu\text{m}^2$ rectangular mask centered at the microring.

Linear characterization

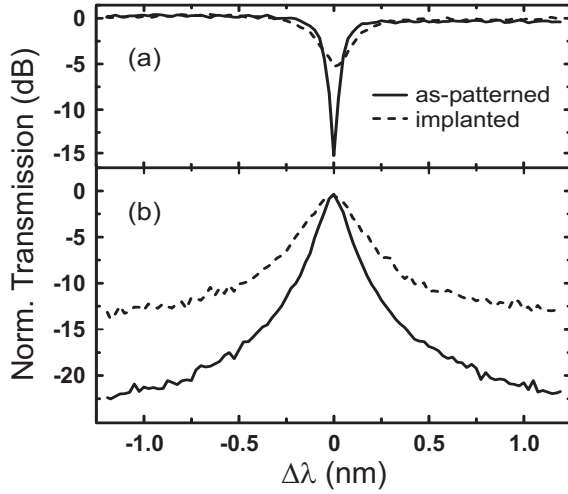


Fig. 1: Transfer function of the investigated microring resonator after EBL patterning (solid lines) and after additional O^+ ion implantation at energy of 120 keV and dose of $1 \times 10^{12} \text{ cm}^{-2}$ (dotted lines). (a) drop port and (b) through port. $\Delta\lambda = \lambda - \lambda_0$, with λ_0 the resonance wavelength.

The linear spectral response of the fabricated device was measured before and after the implantation process. Transmitted light at the through channel (Figure 1(a)) and resonator-coupled light at the drop channel (Figure 1(b)) were measured for TM-polarization (for details of the experimental setup see Ref. 3). The transmission spectrum (through port) of the unimplanted device exhibits a sharp dip of approximately -15 dB at the resonance wavelength $\lambda_0 = 1567.72$ nm. The quality factor of this resonance, defined as $Q = \lambda_0 / \Delta\lambda_{3dB}$, is 11450. In comparison, the transmission spectrum of the implanted microring shows an increase in spectral width and a concomitant decrease in modulation depth. The corresponding Q -factor is about 6200, and in resonance the transmission drops only by about -5 dB. The corresponding maxima measured at the drop channels (Figure 1(b)) exceed the background level by about 22.5 dB and 13 dB for the as-patterned and implanted device, respectively.

Implantation induced defects in the resonator waveguide are assumed to increase the waveguide propagation losses by providing additional light scattering centers. To gain detailed insight into the observed Q -factor decrease, we quantify the microring's photon losses per roundtrip before and after ion implantation. To this end, we fit the analytical transfer function

$$|S_{21}|^2 = \frac{t^2 + t^2\tau^2 - 2t^2\tau \cos \phi}{1 + t^4\tau^2 - 2t^2\tau \cos \phi}, \quad (1)$$

to the respective transmission spectra measured at the through port of the device. Here, t is the symmetric field transmission coefficient at the coupling gaps between resonator and bus waveguides at through and

drop channel, τ the field transmission per resonator roundtrip, and $\phi = 2\pi n_{eff}L/\lambda$ the phase shift per round trip with effective refractive index n_{eff} and resonator length L [15]. The coupling coefficients obtained from these numerical fits are $t_1 = 0.9962$ and $t_2 = 0.9958$ before and after implantation of the device, respectively. Hence, the the implantation process affects the coupling strength between the waveguides and the resonator only marginally. In contrast, the transmission coefficient drops from $\tau_1 = 0.9987$ to $\tau_2 = 0.9908$ as consequence of the implantation process. The corresponding waveguide losses in the resonator $\alpha = -2 \ln(\tau)/L$ increase from 3.6 dB/cm to 25.6 dB/cm – an effect which is expected from additional scattering centers for the light wave propagating in the implanted microring. Nonetheless, the Q -factor of the implanted device is sufficiently large, to allow for optical switching at reasonable carrier densities [6, 7].

Time-resolved switching characteristics

All-optical switching characteristics of the implanted device are investigated in a pump-probe setup which allows for a spectral analysis of the switching process with sub-picosecond resolution (see Fig. 2).

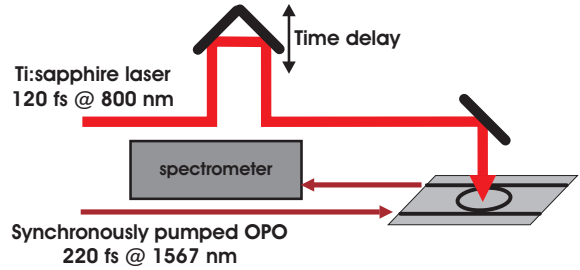


Fig. 2: Schematic illustration of the experimental setup for the time-resolved investigation of the switching process.

For optical excitation, laser pulses of 120 fs duration are derived from a Ti:sapphire oscillator at 800 nm wavelength. These are focussed onto the microring to photogenerate electron-hole pairs in the resonator waveguide by linear absorption. The spectral response of the device is probed with infrared pulses from a synchronously pumped optical parametric oscillator. The pulse length is 220 fs, the central wavelength is adjusted close to the resonance of the microring at $1.567 \mu\text{m}$, and the spectral bandwidth is about 15 nm. These probe pulses are coupled to the device waveguides by a polarization maintaining singlemode fiber. A second singlemode fiber guides the output at the drop channel to a sub-nanometer resolution optical spectrum analyzer. A motorized translation stage provides an adjustable time delay between excitation and probe pulses to temporally resolve the switching dynamics.

Figure 3 shows the temporal evolution of the spectrally resolved intensity measured at the drop channel

of the implanted microring resonator. The spot diameter and pulse energy of the excitation laser are $20\ \mu\text{m}$ and $0.75\ \text{nJ}$. At zero time delay, the resonance of the device clearly shifts to shorter wavelength followed by a red-shift to its initial position within $200\ \text{ps}$ after optical excitation. The resonance shift at $\Delta t = 0$ is accompanied by a decrease of the resonance amplitude and, again, subsequent relaxation to approximately the initial value within the measured time window. Both observations are ascribed to the optical excitation of electron-hole pairs and their fast recombination dynamics. As long as photogenerated free carriers are present in the microring waveguide the resonance wavelength shifts out of equilibrium via the plasma dispersion effect, while the drop port intensity decreases due to an increased free carrier absorption at the infrared probe wavelength.

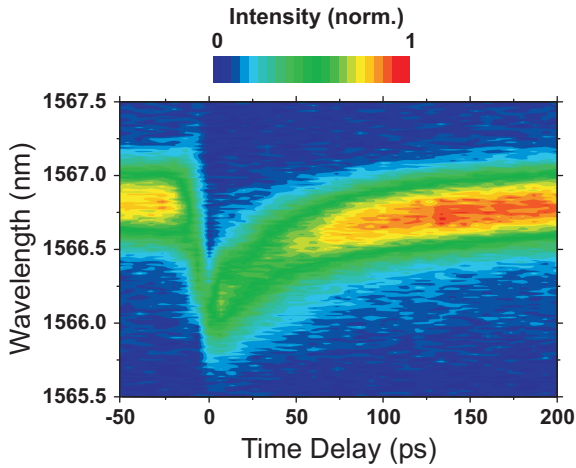


Fig. 3: Spectral response (intensity plot) of the implanted microring resonator measured at the drop channel after optical excitation.

The temporal evolution of the resonance wavelength shift, plotted in Fig. 4(a), is determined by the intrinsic response time of the resonator and the lifetime of photogenerated electron-hole pairs [7, 12]. Although charge carriers are optically excited within a $120\ \text{fs}$ pulse duration, the temporal evolution of the wavelength shift out of resonance at zero time delay is governed by the photon cavity lifetime τ_{cav} . For the investigated resonance of the device, we calculate $\tau_{cav} = \lambda_0 / (2\pi c Q) = 5.2\ \text{ps}$, where c is the vacuum speed of light. A monoexponential numerical fit to the wavelength shift for negative time delays (not shown in Fig. 4(a)) results in $\tau_{cav} = 6.2\ \text{ps}$ which is in close agreement with the cavity photon lifetime calculated from the quality factor. Note here, that $\Delta t = 0$ is defined at the time delay of maximum wavelength shift. At positive time delays, the peak wavelength of the resonance shifts back to its equilibrium position. In this case, the corresponding time constant is determined by the free carrier lifetime $\tau_{e,h}$ in the waveguide. From a monoexponential fit to these data (grey solid line in

Fig. 4(a)), $\tau_{e,h} = 55\ \text{ps}$ is obtained which clearly demonstrates the capability of O^+ -ion implantation to drastically reduce the effective free carrier lifetime in the silicon waveguide. Noteworthy, the free carrier lifetime – measured in the investigated microring device at the chosen implantation dose of $1 \times 10^{12}\ \text{cm}^{-2}$ – corresponds well to published data of O^+ -implanted bulk Si [13]. Note, that an increase of the ion implantation dose is expected to result in a further reduction of the free carrier lifetime where values below $10\ \text{ps}$ are predicted at an implantation dose of about $1 \times 10^{13}\ \text{cm}^{-2}$. In this case, careful attention will have to be paid to a further increase of waveguide propagation losses which will, in turn, decrease the resonator Q -factor and concomitantly increase required switching powers [16].

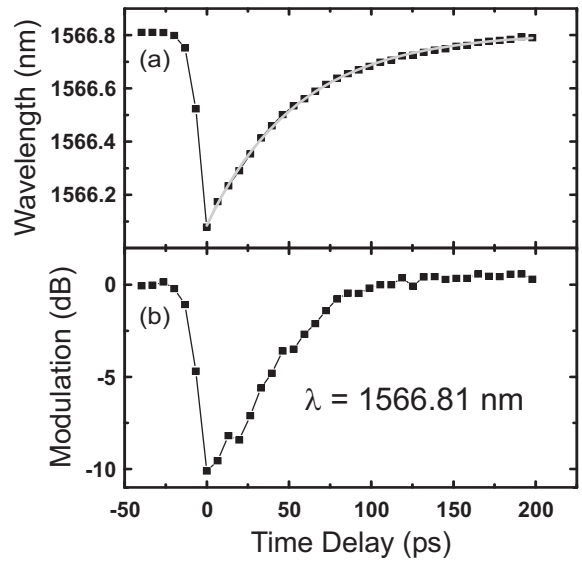


Fig. 4: (a) Time resolved shift of the peak resonance wavelength at the drop waveguide (squares). The grey solid line is an exponential fit to the data for positive time delays. (b) Normalized drop waveguide intensity at the resonance wavelength $\lambda = 1566.81\ \text{nm}$.

For a quantitative spectral analysis of the induced wavelength shift, Fig. 4(a) depicts resonance peak wavelength as a function of time delay. The maximum resonance shift at zero time delay is $\Delta\lambda = -0.74\ \text{nm}$. Considering an effective refractive index $n_{eff} = 2.27$ of the resonator waveguide, this wavelength shift corresponds to a carrier-induced effective refractive index change $\Delta n_{eff} = 1.07 \times 10^{-3}$ or a silicon refractive index change $\Delta n_{Si} = 0.97 \times 10^{-3}$, respectively. A photogenerated charge carrier density of $\Delta N_{e,h} = 2.7 \times 10^{17}\ \text{cm}^{-3}$ is required to induce this refractive index change in an unimplanted silicon microring [5]. From the experimental parameters, i.e. laser spot size, pulse energy, and microring dimensions, and the silicon absorption coefficient $\alpha_{Si} = 1500\ \text{cm}^{-1}$ at $800\ \text{nm}$ wavelength, we estimate an optical excitation density of $\Delta N_{e,h} = 5.5 \times 10^{17}\ \text{cm}^{-3}$ in the resonator waveguides.

The equivalent optical energy absorbed in the microring amounts to 0.75 pJ which corresponds to about one per mill of the laser power incident on the sample. The calculated and experimentally obtained carrier densities differ by only a factor of 2, thus showing good quantitative agreement.

To demonstrate the applicability of the fabricated device as an all-optical switch for a continuous-wave signal beam, Fig. 4(b) shows the temporal evolution of the normalized drop port intensity at the resonance wavelength $\lambda_0 = 1566.81$ nm. At zero time delay, the intensity drops by approximately -10 dB and completely recovers within the following 100 ps. This dynamic response facilitates optical switching at data rates beyond 5 Gbit/s.

Conclusion

In conclusion, we demonstrated the capability of O^+ ion implantation to reduce the free carrier lifetimes in a silicon strip waveguide device. High-speed all-optical light modulation was observed in an SOI microring resonator at a moderate implantation dose. A further increase of the optical modulation frequency, which is essential for future silicon photonic circuits, appears feasible by reducing the free carrier lifetime at higher implantation doses.

Acknowledgments

We thank F. Merget for assistance in sample fabrication. This work has been financially supported by the European Commission within the STREP project "Circles of Light" (Contract No. FP6-034883) and in part within the European Network of Excellence "ePIXnet".

References

- [1] L. Pavesi and G. Guillot (Eds.) "Optical Interconnects: The Silicon Approach", Springer Series in Optical Sciences **119**, (Springer Verlag, Berlin, 2006).
- [2] T. Baehr-Jones, M. Hochberg, C. Walker, and A. Scherer, *Appl. Phys. Lett.* **85**, 3346 (2004).
- [3] J. Niehusmann, A. Vörckel, P. Haring Bolivar, T. Wahlbrink, W. Henschel, and H. Kurz, *Opt. Lett.* **29**, 2861 (2004).
- [4] B.E. Little, S.T. Chu, H.A. Haus, J. Foresi, and J.-P. Laine, *IEEE J. Lightwave Technol.* **15**, 998 (1997).
- [5] R. Soref and B. Bennett, *IEEE J. Quantum Electron.* **23**, 123 (1987).
Phys. Lett. **59**, 3276 (1991).
- [6] V.R. Almeida, C.A. Barrios, R.R. Panepucci, M. Lipson, M.A. Foster, D.G. Ouzonov, and L. Gaeta, *Opt. Lett.* **29**, 2867 (2004).
- [7] V.R. Almeida, C.A. Barrios, R.R. Panepucci, and M. Lipson, *Nature* **431**, 1081 (2004).
- [8] R. Claps, V. Raghunathan, D. Dimitropoulos, and B. Jalali, *Opt. Express* **12**, 2774 (2004).
- [9] H. Rong, A. Liu, R. Jones, O. Cohen, D. Hak, R. Nicolaescu, A. Fang, and M. Paniccia, *Nature* **433**, 292 (2005).
- [10] D. Dimitropoulos, R. Jhaveri, R. Claps, J.C.S. Woo, and B. Jalali, *Appl. Phys. Lett.* **86**, 071115 (2005).
- [11] Q. Xu, B. Schmidt, S. Pradhan, and M. Lipson, *Nature* **435**, 325 (2005).
- [12] S.F. Preble, Q. Xu, B.S. Schmidt, and M. Lipson, *Opt. Lett.* **30**, 2891 (2005).
- [13] F.E. Doany, D. Grischkowsky, and C.-C. Chi, *Appl. Phys. Lett.* **50**, 460 (1987).
- [14] Y. Liu and H.K. Tsang, *Opt. Lett.* **31**, 1714 (2006).
- [15] A. Vörckel, M. Mönster, W. Henschel, P. Haring Bolivar, and H. Kurz, *IEEE Photon. Technol. Lett.* **15**, 921 (2003).
- [16] Q. Xu, V.R. Almeida, and M. Lipson, *Opt. Lett.* **30**, 2733 (2005).